Transport in Porous Media (2019) 130:969–983
https://doi.org/10.1007/s11242-019-01350-7

Long-Term Evolution of Coal Permeability Under Effective Stresses Gap Between Matrix and Fracture During CO_2 Injection

Mingyao Wei[1] · Jishan Liu[2] · Rui Shi[3] · Derek Elsworth[4] · Zhanghao Liu[5]

Received: 11 March 2019 / Accepted: 12 October 2019 / Published online: 24 October 2019

Abstract
Understanding the long-term evolution of coal permeability under the influence of gas adsorption-induced multiple processes is crucial for the efficient sequestration of CO_2, coalbed methane extraction and enhanced coal bed methane recovery. In previous studies, coal permeability is normally measured as a function of gas pressure under the conditions of constant effective stresses, uniaxial strains and constant confining pressures. In all these experiments, an equilibrium state between coal matrix and fracture is normally assumed. This assumption has essentially excluded the effect of matrix–fracture interactions on the evolution of coal permeability. In this study, we hypothesize that the current equilibrium assumption is responsible for the discrepancy between theoretical expectations and experimental measurements. Under this hypothesis, the evolution of coal permeability is determined by the effective stress gap between coal matrix and fracture. This hypothesis is tested through an experiment of CO_2 injection into a coal core under the constant effective stress. In this experiment, the effective stress in the fracture system is unchanged while the effective stress in the matrix evolves as a function of time. In the experiment, the coal permeability was measured continuously throughout the whole period of the experiment (~ 80 days). The experimental results show that the core expands rapidly at the beginning due to the gas injection-induced poroelastic effect. After the injection, the core length remains almost unchanged. But, the measured permeability declines from 60 to 0.48 μD for the first month. It rebounds slowly for the subsequent 2 months. These results indicate that the effective stress gap has a significant impact on the evolution of coal permeability. The switch of permeability from the initial reduction (the first 30 days) to rebound (the subsequent 50 days) suggests a transition of matrix deformation from nearby the fracture wall to further away area. These findings demonstrate that the evolution of coal permeability is primarily controlled by the spatial transformation of effective stresses between matrix and fracture.

Keywords Coal permeability · Gas adsorption · Matrix swelling · Equilibrium state · Effective stress gap

✉ Mingyao Wei
cumtwmy@sina.com

Extended author information available on the last page of the article

1 Introduction

Coal permeability is widely studied due to its importance for a variety of areas such as CO_2 storage in coal seams. Coal swelling due to gas adsorption during CO_2 injection has an important influence on the evolution of permeability (Somerton et al. 1975; Siriwardane et al. 2009; Chen et al. 2011). It is also a common issue for coalbed methane extraction and enhanced coal bed methane recovery. Coal matrix swelling could modify coal permeability. Coal permeability is controlled competitively by effective stresses and matrix swelling during CO_2 injection (Siriwardane et al. 2009). A broad variety of models have been developed to account for the effects of effective stress and swelling (Gray 1987; Seidle et al. 1992; David et al. 1994; Palmer and Mansoori 1996; Shi and Durucan 2004; Cui and Bustin 2005; Robertson and Christiansen 2006; Zhang et al. 2008; Liu et al. 2011; Wang et al. 2012). They have been used to evaluate the evolution of coal permeability for several decades.

Experiments have been undertaken to investigate the evolution of coal permeability under constant confining pressure, constant effective stress and uniaxial strain conditions. In all of experimental observations under constant confining stresses, the permeabilities can be classified into two types: linear and "V" shape (McKee et al. 1987; Harpalani and Schraufnagel 1990; Robertson and Christiansen 2005). In the linear type, permeability increases directly with the injection pressure (Harpalani and Zhao 1989; Harpalani and Schraufnagel 1990; Robertson and Christiansen 2005; Pini et al. 2009; Chen et al. 2011; Wang et al. 2011; Kumar et al. 2012; Wang and Liu 2016). When the confining pressure changes, coal permeability increases monotonously as the effective stresses decrease (Gilman and Beckie 2000; Seidle and Huitt 1995; Robertson and Christiansen 2005; Shi and Durucan 2004; Palmer and Mansoori 1996). The monotonous response of permeability under variable effective stresses is consistent with the theoretical expectation of conventional permeability models. In the "V" type, permeability decreases initially with the increasing of injection pressure, and then rebounds (Kumar et al. 2012; Robertson and Christiansen 2005; Wang et al. 2011). This type response contradicts the theoretical expectation of conventional permeability models.

In addition to experiments under variable effective stresses, coal permeability is also measured under constant effective stresses (Lin et al. 2008; Pan et al. 2010; Chen et al. 2011; Anggara et al. 2016). Our statistical results of these experimental observations show that the permeability ratios decrease as the gas infiltration progresses from fracture wall into matrix (Shi et al. 2018). This gas infiltration causes the time-dependent expansion of the coal matrix which affect in turn the evolution of permeability (Wang et al. 2016). The permeability variation of coal with time under the condition of constant effective stress suggests that the coal matrix–fracture interaction has not reached the final equilibrium state. The experimental results under the field condition of uniaxial strains also show the effect of sorption-induced volumetric strain on the permeability of coal (Mitra et al. 2012; Espinoza et al. 2015). Experimental measurements were normally assumed under the equilibrium state but the observation may suggest that the equilibrium state has not been achieved (Chen et al. 2011; Robertson and Christiansen 2005; Siriwardane et al. 2009; Liu et al. 2016; Zhang et al. 2018).

The suggested inconsistency between assumption and reality, as reviewed above, is also reflected in the strain measurements. Experiments on coal deformation found that methane took nearly months to reach strain equilibrium (Harpalani and Chen 1995; Danesh et al. 2017). The strain equilibrium was associated with gas pressure equilibrium between matrix

and fracture. When the gas pressures reach equilibrium, the adsorption-induced strain and effective stress change-induced strain achieve a steady state. The matrix permeability generally ranges from the order of 1 μD to 10^{-2} nD (Bustin et al. 2012). Therefore, the process of gas transport in the tight matrix is an extremely slow process. In experimental studies (Reucroft and Patel 1986; Seidle and Huitt 1995), extremely long equilibrium time was required from 10 days to months. However, most of the permeability tests published in the literature were conducted within days. For these experiments, gas pressure distribution in the matrix is basically in the non-equilibrium state during the whole measurement process. Thus, all the experimental data were conducted under non-equilibrium conditions. Because they are derived under the equilibrium condition, conventional permeability models cannot be applied to explain the experimental observations. In this study, an experiment was conducted under constant effective stress in fracture system and variable effective stress in matrix system. Permeability was measured continuously for the whole process of permeability evolution from initial to final equilibrium.

2 Experimental Approach

For coal, dual porosity model was widely applied to represent the complex hydro-mechanical coupling behaviors between fracture and matrix. Because fracture permeability is much greater than matrix permeability, the measured permeability can be attributed to the fracture system. Most of the permeability measurements with the steady-state method and transient method are all based on the assumption of equilibrium state. In order to investigate the whole process of fracture permeability evolution from initial to final equilibrium, a permeability experiment with continuous measurements was conducted. It is based on pulse decay technique that takes a short time per measurement. The specific implementation mode of the pressure transient method is shown in Fig. 1. Before the test, a solid metal core was used instead of coal core for leakage measurement. The upstream and downstream of the holder were closed for 48 h

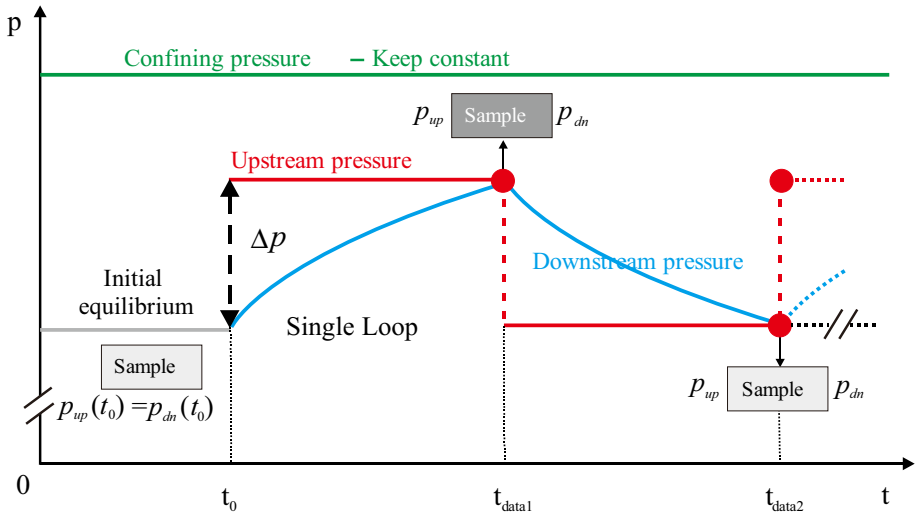

Fig. 1 Schematic diagram of the continuous pressure transient method

after gas was injected. The gas pressure was monitored to determine whether a gas leak occurs. The core is placed into the core holder and then the confining stress is applied. After vacuumed it is flushed with the gas to be used. The injection pressure is kept as a constant for a while (gray line). It can avoid the leakage effect of upstream side on the measurement accuracy. It is considered that the pressure distribution in the fracture system is equilibrated at this stage (light gray rectangular, $p_{up}=p_{dn}$). Then, a pressure increment (Δp, e.g., 0.3 MPa) is applied to the upstream reservoir. The upstream is connected to a gas pressure controller which can maintain the upstream pressure at pre-assigned pressures in each loop (red line). The upstream pressure is controlled automatically. This is much more convenient for the long-term test. It is different from the traditional pressure transient method which upstream pressure decreases. Because the gas transports through the coal to the downstream reservoir under the pressure driven. The downstream pressure (blue line) changes before reaching upstream pressure. There is always a pressure difference between the upstream and the downstream. The collected decay rate pressure difference is used to evaluate the permeability. The time from t_0 to t_{data1} is one loop for permeability measurement. After the end of each loop, the upstream pressure is switched periodically to continue the subsequent loops. These loops continue as long as the calculated permeability unchanged.

The transient method of Brace (Brace et al. 1968) is widely used to conduct the gas flow experiments in the low permeability cores. But the difference between our method and the Brace method is that the upstream pressure is kept constant in each one loop in our method. The upstream pressure does not deplete as the gas transfer to the downstream. The upstream pressure can be controlled by the computer program automatically. The differential pressure between upstream and downstream was continuously measured and recorded. This pressure decay is combined with the vessel volumes in the analysis to relate the flow through the core and thus determine the permeability. The pressure decay curve can be modeled as:

$$\frac{P_{up}(t)-P_{dn}(t)}{P_{up}(t_0)-P_{dn}(t_0)}=e^{-vt} \tag{1}$$

$$v=\frac{kA}{\mu\beta L}\left(1/V_{up}+1/V_{dn}\right) \tag{2}$$

where $p_{up}(t)-p_{dn}(t)$ is the pressure difference between the upstream and downstream reservoirs at time t, (Pa), $(p_{up}(t_0)-p_{dn}(t_0))$ is the initial pressure difference between the upstream and downstream reservoirs at time t_0, (Pa), υ is the slope of the line when plotting the pressure decay $p_{up}(t)-p_{dn}(t)$ on semi-log paper against time, L is the core length (cm), A is the cross-section area of the core (cm^2), μ is the dynamic viscosity (cp), β is the compressibility of the gas, and V_{up} and V_{dn} are the volumes of the upstream reservoir and downstream reservoir, respectively (cm^3). Because the upstream pressure is maintained as constant within one loop, V_{up} tends to infinity. A simplified expression of permeability can be derived from Eq. (2) as (Heller et al. 2014).

$$k=\frac{v\mu\beta LV_{dn}}{A} \tag{3}$$

In each loop, the permeability is calculated with Eq. (3). For the full experimental process, the permeability evolution of the core can be captured continuously.

3 Experimental Specimen, Apparatus, and Procedures

3.1 Coal Core

The coal core was obtained from the exposed surface of an underground mine located in Henan Province in China as shown in Fig. 2. The burial depth is − 310 m with burial stress of 6.1 MPa. The coal is categorized as high-volatile bituminous. The physical dimension of the coal core is 50 mm in diameter by 100 mm in length. The fracture distribution of the core was investigated by using 3D-CT Scan machine (Sanying Precision Instruments Ltd.). The resolution of CT scanning is about 30 μm. The images directly obtained by CT contain a certain level of noise. We select the median filtration method to smooth the boundary (Gallagher and Wise 1981). In order to better divide the fractures and matrix, between-class variance maximization algorithm was selected to make the image segmentation process accurately (Baradez et al. 2004). It can be seen that the fracture is parallel to the axial direction, that is parallel to the gas flow direction in the experiment.

3.2 Apparatus

A core flow apparatus, unconventional gas (UG) permeability test system, with the data processing software was used for coal permeability measurements in this study. A schematic diagram of the experimental apparatus is shown in Fig. 3. The central part of the

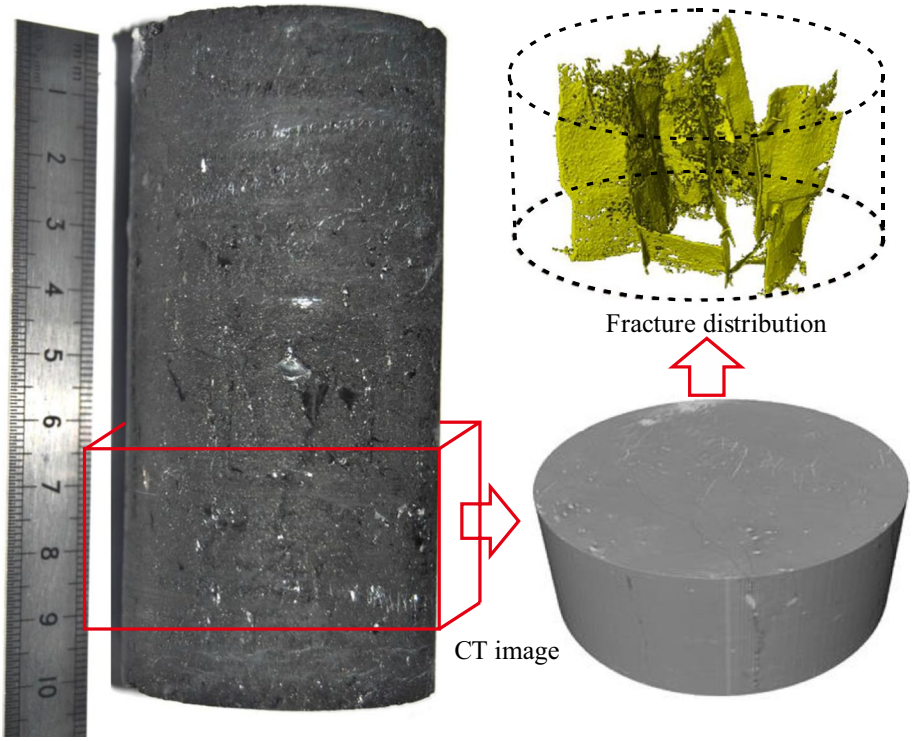

Fig. 2 Coal core after preparation and fractures distribution

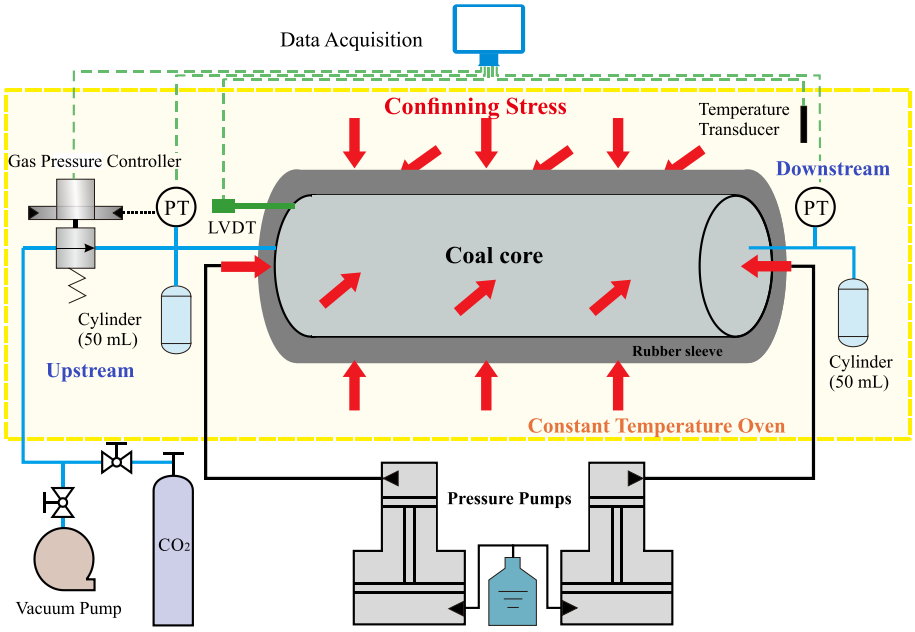

Fig. 3 Schematic of experimental apparatus for measurement of permeability and axial displacement

apparatus is the high-pressure chamber, where confining pressure is loaded to simulate the underground conditions. It's capable of accepting membrane-sheathed cylindrical cores (5.0 cm diameter). The volume of the downstream reservoir is 50 mL. Coal core encased in the rubber sleeve is jacketed in a core holder. The core is isolated from the confining fluid by the sleeve made of butyl rubber, and pore pressure is controlled independently of the confining pressure. Axial stress up to 70 MPa and confining (radial) stresses up to 40 MPa are independently applied by using two pumps. Upstream pressure is controlled by an electro-pneumatic actuator connecting to a pneumatically actuated regulator. The gas pressure controller has an accuracy of 0.1% of full scale. The gas leakage has no effects on the results during a long-term experiment because of the sealed downstream side and constant pressure on the upstream side. During the experiment, the injection pressure of upstream is kept at a constant. The gas is supplied from the gas cylinder to keep the pressure constant. It can avoid the leakage of the upstream side on measurement accuracy. The downstream gas pipelines are short. The leakage effects can be neglected in each test loop. And gas pressure is initialized before the next loop. So, the leakage effects can be neglected during the long-term tests.

Measurements of the axial displacement of cylindrical cores are commonly performed with linear variable differential transformers (LVDT) (Espinoza et al. 2014; Chen et al. 2015; Wang et al. 2016). One set of LVDT is placed at one side of the core to measure the displacement change. All transducers (temperature, pressure, and displacement transducers) are connected to a computer to automatically record the experimental data. All parts of the apparatus are located in a temperature-controlled cabinet where the temperature can be maintained constant with a deviation of ± 0.5 °C.

3.3 Experimental Procedure

The following details the experimental steps used to conduct such a study.

Step 1 Coal core was placed in an oven at 45 °C for 12 h before being placed in the typical Hassler core holder with measurement of axial strain. Note that it is not a vacuum oven. Then, the core weight was measured.
Step 2 Coal core was jacketed in the core holder. To independently test the effects of adsorption swelling on permeability, it is necessary to keep the gas pressure and confining stress constant. Both confining pressure (6.0 MPa) and axial stresses (6.0 MPa) were applied at a slow rate to establish initial conditions and then kept constant. Prior to the test, the core-reservoir system was vacuum desaturated to evacuate air from the system for 24 h. The temperature was maintained at 23 °C during the whole period of the experiment.
Step 3 Absorbing gas (CO_2) was used as the fluid medium in the experiment. Then, the core was exposed to CO_2 after upstream and downstream injection. After achieving the desired pore pressure level, both upstream pressure and downstream were fixed at 3 MPa for five minutes. In this stage, fracture pressure was nearly equilibrated because the downstream pressure was stable at this moment.
Step 4 The confining stress was kept constant. Coal permeability was measured continuously using the method introduced in Sect. 2. The single loop of measurement was last for 1 h. The procedure was repeated for a step-wise periodically lasting for 88 days. The upstream pressure was controlled by the preprogrammed command sequences, which guide the actuated regulator.
Step 5 After the permeability test, the coal core was taken out. The core was sealed with plastic film to keep dry. The change in coal mass from the moment of taking the core out of the cell was recorded once every 2 days in an attempt to derive the change in adsorbed mass.

4 Experimental Results

Because the experiment was conducted for a long period of time, large amounts of data were collected by the computer. A MATLAB code was developed to process the experimental data. There are a few invalid data calculated by MATLAB code. It is because of the failing dissociation of each loop from successive data. At first, some invalid data has to be removed. Then, each loop of pressure data was sorted. Then, the permeability was obtained by fitting the slope of the pressure difference between the upstream and downstream sides. There are 2210 data of permeability was calculated at last. The measured data (Upstream pressure, downstream pressure, axial displacement, temperature, confining pressure) and calculated permeability are shown in Fig. 4. Note that there is still one experiment presented in this paper due to the time-consuming. So the influence of coal characteristic on permeability evolution is not considered in this paper.

As shown in Fig. 4, the permeability and axial displacement both varied significantly, although the confining pressure and gas pressure were kept constant in the experiment. The pore pressure is 0 MPa at zero of X-axis in Fig. 4, then it increased to 3 MPa instantly. The axial displacement increases rapidly as gas injected into the core. After a few hours,

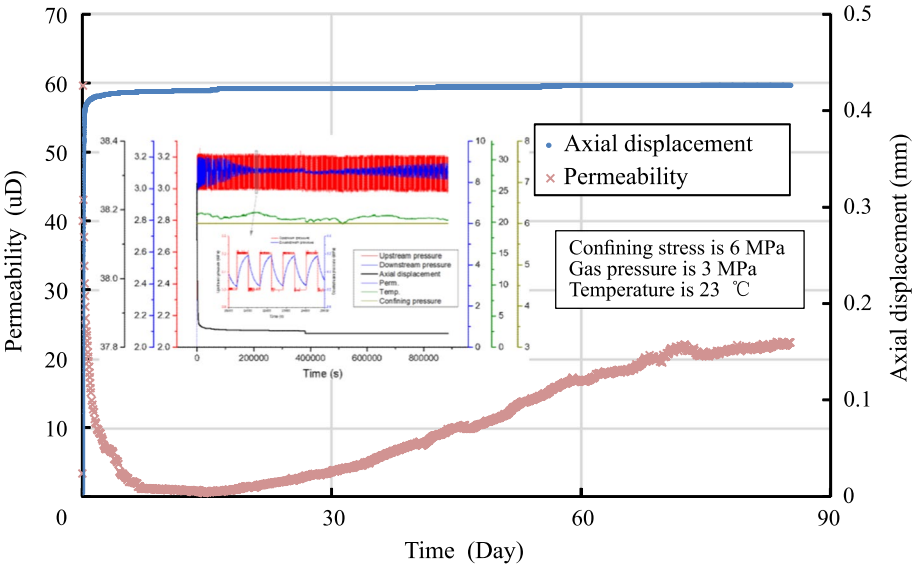

Fig. 4 The experimental data of permeability and axial displacement

the rate of axial displacement growth slows down. Over last 80 days, it remains about the same. The maximum displacement is 0.43 mm, corresponding to the strain of 0.43% in the axial direction. In comparison, the change tendency in permeability is totally different. The first three loops of permeability tests show the increase in permeability. The highest value of permeability is 60 μD. After then, it drops down from the highest to lowest in 10 days. It finally declines to 0.48 μD, which is 125 times reduction. It remains constant for a few days. Then, it begins to rebound slowly and last for the next 2 months. At the last, the permeability remains almost unchanged.

We assume that the mass of the adsorbed gas is zero before gas injection. It shows that the gas mass in the core reduced by 9.46 g in 18 days from the moment it was taken out of the cell as shown in Fig. 5. The adsorbed gas in the matrix was mainly not released at that moment. The mass decreased when the core was exposed to air. During this period, the adsorbed gas desorbed to free gas from the coal matrix to fracture. At last, the mass reduced to the value prior to the experiment. It took about 18 days for the pressure in the fracture to re-equilibrate with the pressure in the matrix.

5 Analyses and Discussions

5.1 Nonsynchronous Deformation of Fracture and Matrix

Since the core was confined by a constant confining pressure, the decrease in effective stress results in the core expansion after CO_2 injection. The adsorption-induced swelling also leads to the increased axial displacement. Therefore, both effective stress and adsorption strain account for the core deformation. In order to evaluate the effect of these two factors on core deformation, a numerical dual-permeability model was built. It was assumed

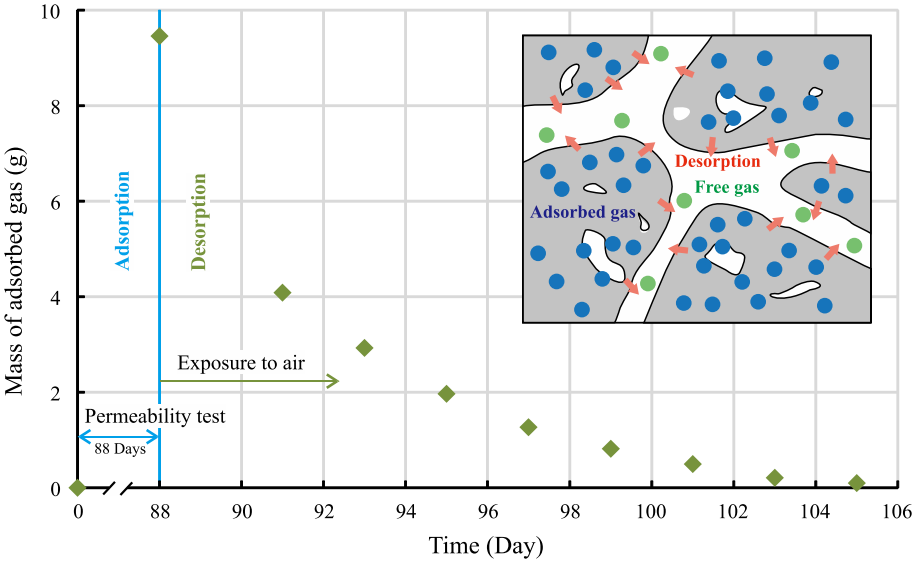

Fig. 5 Mass changes of adsorbed CO_2

that the gas in the matrix exists in both adsorption and free phase. There is only free gas in the fracture. The gas adsorption follows the Langmuir equation. The gas flow in the coal matrix and fracture follows the Darcy's law. The gas mass balance equation in the matrix can be expressed as (Wei et al. 2018):

$$\frac{\partial}{\partial t}\left(\phi_{\mathrm{m}} P_{\mathrm{m}} \frac{M}{RT} + \left(1-\phi_{\mathrm{m}}\right)\rho_{\mathrm{s}}\rho_{\mathrm{a}} \frac{L_{\mathrm{a}} P_{\mathrm{m}}}{P_{\mathrm{m}} + L_{\mathrm{b}}}\right) + \nabla\left(-\frac{M}{RT} P_{\mathrm{m}} \frac{k_{\mathrm{m}}}{u} \nabla P_{\mathrm{m}}\right) = -Q_{\mathrm{mf}} \tag{4}$$

where ϕ_{m} is the porosity of coal matrix, P_{m} is pore pressure in the matrix, M is the molar mass, R is the gas constant, T is the absolute temperature in Kelvin. $_{\mathrm{s}}$ is coal density, $_{\mathrm{a}}$ is gas density at atmospheric pressure, L_{a} represents the Langmuir volume constant, L_{b} represents the Langmuir pressure, u is gas viscosity, Q_{mf} is the mass transfer rate between matrix and fracture.

The mass exchange between matrix and fracture is defined by a coupling term Q_{mf}:

$$Q_{\mathrm{mf}} = a_{\mathrm{mf}} D_{\mathrm{mf}} \left(\rho_{\mathrm{m}} - \rho_{\mathrm{f}}\right) \tag{5}$$

where a_{mf} is a shape factor, D_{mf} is the diffusion coefficient.

Darcy flow is used to define flow in fractures. The gas mass balance equation in the fracture is given as:

$$\frac{\partial}{\partial t}\left(\phi_{\mathrm{f}} P_{\mathrm{f}} \frac{M}{ZRT}\right) - \frac{\rho_{\mathrm{f}} k_{\mathrm{f}}}{u} \nabla P_{\mathrm{f}} = Q_{\mathrm{mf}} \tag{6}$$

where ϕ_{f} is the porosity of natural fracture, k_{f} is the permeability of fracture, ϕ_{f0} is the initial porosity of natural fracture, k_{f0} is the initial permeability of natural fracture, P_{f} is the gas pressure in the fracture, $_{k}$ is the gas density in fracture system.

The parameters used in the simulation are listed in Table 1. The permeabilities of matrix and fracture were back-calculated according to the experimental results. Other

Table 1 Parameters for simulation

Parameter	Value
Density of coal, ρ_s	1400 kg/m^3
Density of CO_2 at standard condition, ρ_a	0.71 kg/m^3
Viscosity of CO_2, μ	1.84×10^{-5} Pa·s
Langmuir pressure constant, L_a	0.015 m^3/kg
Langmuir volume constant, L_b	6.109 MPa
Porosity of matrix, ϕ_m	0.021
Permeability of matrix, k_m	1×10^{-21}m^2
Porosity of fracture, ϕ_f	0.014
Permeability of fracture, k_f	1×10^{-17} m^2
Shape factor, a_{mf}	1
Diffusion coefficient, D_{mf}	1×10^{-9} m/s
Diameter of numerical model	5 cm
Height of numerical model	10 cm

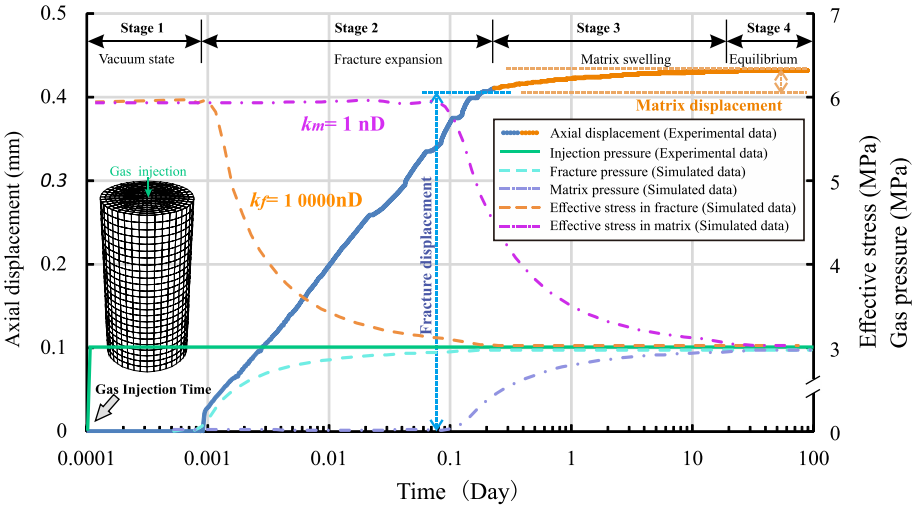

Fig. 6 Measured axial displacement variation in response to the simulated effective stress

parameters are obtained from the literature (Wu et al. 2010). The governing equations have been implemented into and solved by COMSOL Multiphysics. The modeling results are shown in Fig. 6. These results reveal the difference of pressure distributions and the transformation of effective stresses between fracture and matrix. The axial displacement curve can be divided into four stages:

(1) Stage 1: Vacuum State. It lasts a very short period right after the gas injection. The fracture and matrix are in the vacuum stage. In this stage, the effective stresses are still unchanged. The gas fills in the fracture during this stage.

(2) Stage 2: Core Expansion. As the gas filtration into the fracture progresses, the axial displacement increases rapidly. Under the condition of constant confining pressure, effective stress decreases due to the increase in gas pressure. In this stage, the effective stress in the fracture decreases while that in the matrix remains relatively unchanged. It confirms that the rapid deformation of the core is due to the fracture expansion.
(3) Stage 3: Matrix Swelling. In this stage, the effective stress in the matrix decreases as the gas diffuses from the fracture into the matrix. As a result, coal matrix swells in this stage. The gas diffusion leads to a slow displacement growth over the next 2 months of the experiment. But, the increase in axial displacement is quite small comparing with the Stage 2.
(4) Stage 4: Stable Stage. At the last stage, the axial displacement remains unchanged for the later 60 days. The effective stress in both fracture and matrix is stable. A new equilibrium state between matrix and fracture has been reached.

Due to the high permeability in the fracture, the gas flows rapidly within the fracture after gas injection. The gas pressure in the fracture increases in the early stage compared to the gas pressure in the matrix. When the gas reaches the fracture wall and diffuses into matrix, the gas pressure in the matrix begins to rise. Therefore, the gas pressure within the matrix is generally lower than the pressure within the fracture before the final equilibrium state. According to the Terzaghi's principle, effective stress should decrease with the increase in gas pressure when the total stress is constant. It is obvious that there exists a time difference between the change of effective stress in the fracture and that in the matrix. Since the pressure distribution in the matrix changes from non-uniform (early stages) to uniform (final stage), the adsorption-induced swelling deformation also transforms from localization in the vicinity of the fracture compartment to globalization (the whole core).

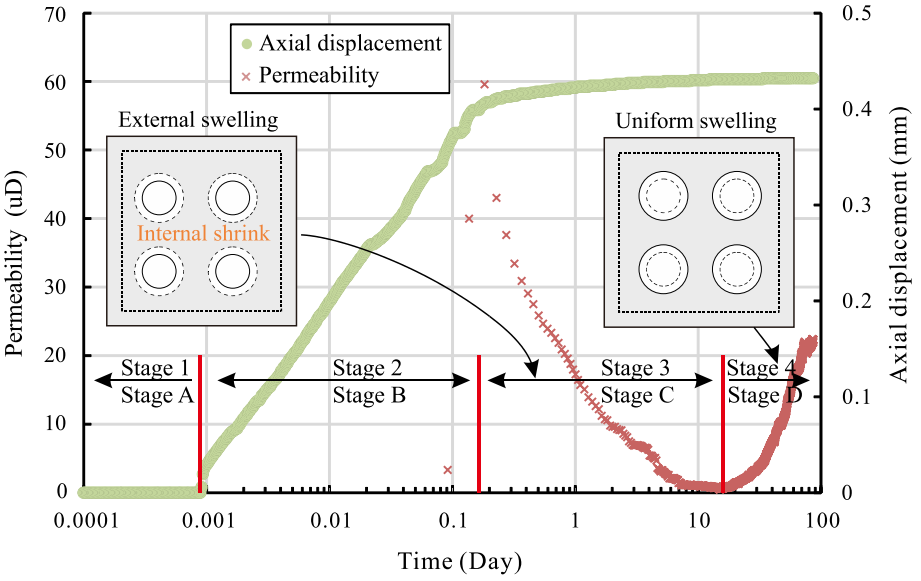

Fig. 7 Illustration of the corresponding relation between displacement and permeability

5.2 Relation Between Core Deformation and Permeability Evolution

The corresponding relation between axial displacement and coal permeability is illustrated in Fig. 7. It is obvious that coal permeability also experiences four stages:

(1) Initial Equilibrium Stage. This is supposed to correspond to the vacuum stage.
(2) Permeability Increase Stage. This is supposed to correspond to the fracture expansion stage;
(3) Permeability Reduction Stage. This is supposed to correspond to the matrix swelling stage.
(4) Permeability Stabilization Stage. This is supposed to correspond to the stable deformation stage.

As shown in Fig. 7, the four stages of coal permeability evolution do not match well with the four stages of axial displacement evolution. For example, coal permeability decreases significantly while the measured axial displacements at Stage 3 are almost ignorable. This inconsistency is due to the fact that coal permeability evolution is determined by the transformation of the internal deformation in the vicinity of the fracture wall and the overall deformation of the core as measured. This transformation corresponds to the transfer of effective stresses between fracture and matrix as discussed in the section above.

6 Conclusion

In this study, a long-term experiment was conducted to measure the evolution of coal permeability under the influence of gas injection. Based on the experimental observations of coal permeability evolution and the corresponding theoretical analysis, the following conclusions can be drawn:

(1) The evolution of coal permeability does not correspond well with the external deformation of coal core as measured. It is determined by the transformation of the local deformation as gas diffuses from the fracture wall into the matrix and the overall deformation as gas spreads all over the coal core.
(2) The effective stress gap between matrix and fracture is primarily controlled by the gas diffusion-induced non-uniform matrix swelling. When the swelling deformation of the matrix is localized in the vicinity of the fracture wall, the fracture opening is reduced by the swelling deformation. At this stage, the coal permeability is controlled primarily by the internal deformation. When the swelling deformation expands throughout the whole core, the permeability change switches from one mode to another.
(3) These findings suggest that coal permeability models, as developed on the basis of overall deformation, may not reflect the true mechanism of deformation transformation from internal mode to external one.

Acknowledgments This work was supported by the National Key Research and Development Program (2017YFC0804400), the Fundamental Research Funds for the Central Universities (2015XKZD03),the Program for Changjiang Scholars and Innovative Research Team in University (IRT_17R103), and the Priority Academic Program Development of Jiangsu Higher Education Institutions. These sources of support

are gratefully acknowledged. We also thank Jianhong Kang for constructive comments during the review process.

References

Anggara, F., Sasaki, K., Sugai, Y.: The correlation between coal swelling and permeability during CO_2 sequestration: a case study using Kushiro low rank coals. Int. J. Coal Geol. **166**, 62–70 (2016)

Baradez, M.O., Mcguckin, C.P., Forraz, N., Pettengell, R., Hoppe, A.: Robust and automated unimodal histogram thresholding and potential applications. Pattern Recogn. **37**(6), 1131–1148 (2004)

Brace, W.F., Walsh, J., Frangos, W.: Permeability of granite under high pressure. J. Geophys. Res. **73**, 2225–2236 (1968)

Bustin, A.M.M., Bustin, R.M., Russel-Houston, J.: Horseshoe canyon and belly river coal measures, south central Alberta: part 2—modeling reservoir properties and producible gas. B. Can Pet Geol. **59**, 235–260 (2012)

Chen, Z.W., Pan, Z.J., Liu, J.S., Connell, L.D., Elsworth, D.: Effect of the effective stress coefficient and sorption-induced strain on the evolution of coal permeability: experimental observations. Int. J. Greenh. Gas Control **5**(5), 1284–1293 (2011)

Chen, D., Pan, Z.J., Ye, Z.H.: Dependence of gas shale fracture permeability on effective stress and reservoir pressure: model match and insights. Fuel **139**, 383–392 (2015)

Cui, X., Bustin, R.M.: Volumetric strain associated with methane desorption and its impact on coalbed gas production from deep coal seams. AAPG Bull. **89**, 1181–1202 (2005)

Danesh, N.N., Chen, Z., Connell, L.D., Kizil, M.S., Pan, Z., Aminossadati, S.M.: Characterisation of creep in coal and its impact on permeability: an experimental study. Int. J. Coal Geol. **173**, 200–211 (2017)

David, C., Wong, T.F., Zhu, W., Zhang, J.: Laboratory measurement of compaction induced permeability change in porous rocks: implications for the generation and maintenance of pore pressure excess in the crust. Pure. Appl. Geophys. **143**, 425–456 (1994)

Espinoza, D., Vandamme, M., Pereira, J.-M., Dangla, P., Vidal-Gilbert, S.: Measurement and modeling of adsorptive–poromechanical properties of bituminous coal cores exposed to CO_2: adsorption, swelling strains, swelling stresses and impact on fracture permeability. Int. J. Coal Geol. **134**, 80–95 (2014)

Espinoza, D.N., Pereira, J.-M., Vandamme, M., Dangla, P., Vidal-Gilbert, S.: Desorption-induced shear failure of coal bed seams during gas depletion. Int. J. Coal Geol. **137**, 142–151 (2015)

Gallagher, N., Wise, G.: A theoretical analysis of the properties of median filters. IEEE Trans. ASSP. **29**, 1136–1141 (1981)

Gilman, A., Beckie, R.: Flow of coalbed methane to a gallery. Trans. Porous Media. **41**, 1–16 (2000)

Gray, I.: Reservoir engineering in coal seams: part 1—the physical process of gas storage and movement in coal seams. Reserv Eng. **2**(1), 28–34 (1987)

Harpalani, S., Chen, G.: Estimation of changes in fracture porosity of coal with gas emision. Fuel **74**(10), 1491–1498 (1995)

Harpalani, S., Schraufnagel, R.A.: Shrinkage of coal matrix with release of gas and its impact on permeability of coal. Fuel **69**, 551–556 (1990)

Harpalani, S., Zhao, X.: The unusual response of coal permeability to varying gas pressure and effective stress. The 30th US Symposium on Rock Mechanics (USRMS). American Rock Mechanics Association. (1989)

Heller, R., Vermylen, J., Zoback, M.: Experimental investigation of matrix permeability of gas shales. AAPG Bull. **98**(5), 975–995 (2014)

Kumar, H., Elsworth, D., Liu, J.S., Pone, D., Mathews, J.P.: Optimizing enhanced coalbed methane recovery for unhindered production and CO_2 injectivity. Int. J. Greenh. Gas Con. **11**(6), 86–97 (2012)

Lin, W., Tang, G.-Q., Kovscek, A.R.: Sorption-induced permeability change of coal during gas-injection processes. Reserv. Eval. Eng. **11**, 792–802 (2008)

Liu, J.S., Wang, J.G., Chen, Z.W., Wang, S., Elsworth, D., Jiang, Y.J.: Impact of transition from local swelling to macro swelling on the evolution of coal permeability. Int. J. Coal Geol. **88**, 31–40 (2011)

Liu, Q.Q., Cheng, Y.P., Ren, T., Jing, H.W., Tu, Q.Y., Dong, J.: Experimental observations of matrix swelling area propagation on permeability evolution using natural and reconstituted samples. J. Nat. Gas Sci. Eng. **34**, 680–688 (2016)

McKee, C.R., Bumb, A.C., Koeing, R.A.: Stress-dependent permeability and porosity of coal. International coalbed methane symposium. **3**(1), 81–91 (1987)

Mitra, A., Harpalani, S., Liu, S.M.: Laboratory measurement and modeling of coal permeability with continued methane production: part 1—laboratory results. Fuel **94**(110), 116 (2012)

Palmer, I., Mansoori, J.: How permeability depends on stress and pore pressure in coalbeds: a new model. SPE Reserv. Eval. Eng. **1**(6), 539–544 (1996)
Pan, Z.J., Connell, L.D., Camilleri, M.: Laboratory characterisation of coal reservoir permeability for primary and enhanced coalbed methane recovery. Int. J. Coal Geol. **82**, 252–261 (2010)
Pini, R., Ottiger, S., Burlini, L., Storti, G., Mazzotti, M.: Role of adsorption and swelling on the dynamics of gas injection in coal. J. Geophys. Res. Solid Earth. **114**, B04203 (2009)
Robertson, E.P., Christiansen, R.L.: Measurements of sorption-induced strain. Presented at the 2005 International Coalbed Methane Symposium, Tuscaloosa, Alabama, 17–19 May, Paper 0532 (2005)
Robertson, E.P., Christiansen, R.L.: A permeability model for coal and other fractured, sorptive-elastic media. SPE J. **13**(3), 314–324 (2006)
Reucroft, P.J., Patel, H.: Gas-induced swelling in coal. Fuel **65**, 816–820 (1986)
Seidle, J.P., Huitt, L.G.: Experimental measurement of coal matrix shrinkage due to gas desorption and implications for cleat permeability increase. In: SPE International Meeting on Petroleum Engineering, Beijing, China, 14–17 November. SPE 30010 (1995)
Seidle, J.P., Jeansonne, M.W., Erickson, D.J.: Application of matchstick geometry to stress dependent permeability in coals. In: SPE 24361 SPE Rocky Mountain Regional Meeting Held in Casper, Wyoming, USA, 18–21 May (1992)
Shi, J.Q., Durucan, S.: Drawdown induced changes in permeability of coalbeds: a new interpretation of the reservoir response to primary recovery. Trans. Porous Med. **56**(1), 1–16 (2004)
Shi, R., Liu, J.S., Wei, M.Y., Elsworth, D., Wang, X.M.: Mechanistic analysis of coal permeability evolution data under stress-controlled conditions. Int. J. Rock Mech, Min (2018). **(In revision)**
Siriwardane, H., Haljasmaa, I., Mclendon, R., Irdi, G., Soong, Y., Bromhal, G.: Influence of carbon dioxide on coal permeability determined by pressure transient methods. Int. J. Coal Geol. **77**(1), 109–118 (2009)
Somerton, W.H., Söylemezoglu, I.M., Dudley, R.C.: Effect of stress on permeability of coal. Int. J. Rock Mech. Min. Sci. Geomech. Abst. **12**(5–6), 129–145 (1975)
Wang, Y., Liu, S.M.: Estimation of pressure-dependent diffusive permeability of coal using methane diffusion coefficient: laboratory measurements and modeling. Energy Fuels **30**(11), 8968–8976 (2016)
Wang, S., Elsworth, D., Liu, J.S.: Permeability evolution in fractured coal: the roles of fracture geometry and water-content. Int. J. Coal Geol. **87**, 13–25 (2011)
Wang, S., Elsworth, D., Liu, J.: A mechanistic model for permeability evolution in fractured sorbing media. J. Geophys. Res. Solid Earth **117**, B06205 (2012)
Wang, C.G., Liu, J.S., Feng, J.T., Wei, M.Y., Wang, C.S., Jiang, Y.J.: Effects of gas diffusion from fractures to coal matrix on the evolution of coal strains: experimental observations. Int. J. Coal Geol. **162**, 74–84 (2016)
Wei, M.Y., Liu, J.S., Elsworth, D., Wang E.Y.: Triple porosity modelling for the simulation of multi-scale flow mechanisms in shale reservoirs. Geofluids, 6948726 (2018)
Wu, Y., Liu, J.S., Elsworth, D., Chen, Z.W., Connell, L., Pan, Z.J.: Dual poroelastic response of coal seam to CO_2 injection. Int. J. Greenh. Gas Con. **4**(4), 668–678 (2010)
Zhang, H.B., Liu, J.S., Elsworth, D.: How sorption-induced matrix deformation affects gas flow in coal seams: a new FE model. Int. J. Rock Mech. Min. Sci. **45**(8), 1226–1236 (2008)
Zhang, S.W., Liu, J.S., Wei, M.Y., Elsworth, D.: Coal permeability maps under the influence of multiple coupled processes. Int. J. Coal Geol. **187**, 71–82 (2018)

Affiliations

Mingyao Wei[1] · Jishan Liu[2] · Rui Shi[3] · Derek Elsworth[4] · Zhanghao Liu[5]

[1] National and Local Joint Engineering Laboratory of Internet Application Technology on Mine, IoT Perception Mine Research Center, China University of Mining and Technology, Xuzhou, Jiangsu 221116, China

[2] School of Engineering, The University of Western Australia, 35 Stirling Highway, Perth, WA 6009, Australia

[3] Key Laboratory of Tectonics and Petroleum Resources, China University of Geosciences, Wuhan 430074, China

[4] Department of Energy and Mineral Engineering, G3 Center and Energy Institute, The Pennsylvania State University, University Park, PA 16802, USA

[5] State Key Laboratory of Geomechanics and Geotechnical Engineering, Institute of Rock and Soil Mechanics, Chinese Academy of Sciences, Wuhan 430071, China